Contribution from the Department of Chemistry, D-006, University of California at San Diego,
La Jolla, California 92093, and Nicolet Instrument Corporation, Madison, Wisconsin 53711-0370

Synthesis and Molecular Structure of 1,4-Diphenyltetrazenido Complexes of Bis(phosphine)nickel, -palladium, and -platinum

Soon W. Lee,[1a] Glenn A. Miller,[1a] Charles F. Campana,[1b] and William C. Trogler*[1a]

Received September 15, 1987

The dichlorobis(phosphine)metal complexes $\mathrm{NiCl_2(PPh_2Me)_2}$, *cis*-$\mathrm{PdCl_2(PEt_3)_2}$, and *cis*-$\mathrm{PtCl_2(PEt_3)_2}$ react with $\mathrm{[Li(THF)_x]_2[PhNN{=}NNPh]}$ (I) to yield crystalline materials of formula $\mathrm{Ni\{N(Ph)\underset{\cdots}{-}N\underset{\cdots}{-}N\underset{\cdots}{-}NPh\}(PPh_2Me)_2}$ (II), $\mathrm{Pd\{N(Ph)N{=}NNPh\}(PEt_3)_2}$ (III), and $\mathrm{Pt\{N(Ph)N{=}NNPh\}(PEt_3)_2}$ (IV), respectively. Their crystal structures were determined through X-ray diffraction at room temperature: II crystallizes in the monoclinic system, space group $C2/c$, with lattice constants $a = 23.556$ (3) Å, $b = 9.044$ (1) Å, $c = 17.892$ (3) Å and $\beta = 114.70$ (3)°, with $Z = 4$; III crystallizes in the monoclinic system, space group $P2_1/c$, with lattice constants $a = 12.904$ (3) Å, $b = 13.405$ (4) Å, $c = 16.670$ (4) Å, and $\beta = 112.01$ (3)°, with $Z = 4$; IV crystallizes in the tetragonal system, space group $P\bar{4}2_1c$, with lattice constants $a = 12.253$ (1) Å and $c = 17.803$ (4) Å, with $Z = 4$. Least-squares refinement of the structures led to R factors of 0.055 (II), 0.050 (III), and 0.044 (IV). The coordination sphere of Ni can be described as a tetrahedron distorted toward a square plane, and those of Pd and Pt can be described as square planes distorted toward tetrahedral structures. All three complexes are highly colored and decompose on irradiation at 290–340 nm. Electrochemical studies show that III displays a quasi-reversible reduction and III and IV display irreversible reductions, suggesting that the acceptor orbital might be localized on the tetraazadiene ring.

Transition-metal tetraazadiene complexes have been synthesized by coupling reactions between either an organic azide ($\mathrm{RN_3}$) or a diazonium salt ($\mathrm{RN_2^+}$) and a metal complex in a low oxidation state,[2] because the free tetraazadiene ligands were unavailable.[3] Since 1967 several transition-metal tetraazadiene complexes have been reported, including derivatives of Ni, Pt, Co, Ir, Rh, and Fe.[2] The $\mathrm{N_4R_2}$ ligand in these compounds is a flexible ligand that can be viewed as either a neutral four-electron σ-donor (A) group or an anionic four-electron donor (B). In structurally characterized complexes with transition metals both bonding modes have been observed with either two or one short N–N bond in the ligand backbone. An alternative molecular orbital description of the bonding views A as a ligand of strong π-acid character. Back-bonding from the metal to the lowest ligand π-acceptor orbital (C) would induce the bond length variation found in structure B. This description also helps explain the short M–N bond lengths found in complexes with structures intermediate between A and B, since M–N π bonding would contribute multiple-bond character. It is worth noting that only late-transition-metal complexes of tetraazadienes have been prepared, which may reflect the importance of metal to ligand back-bonding.

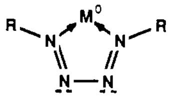

A

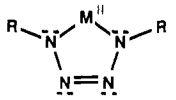

B

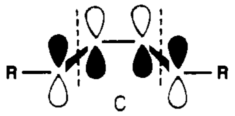

C

To develop the chemistry of metal tetraazadiene complexes, it would be desirable to have a general method for their syntheses. The coupling reactions used previously are erratic because they require a second mole of reagent to intercept an unstable nitrene intermediate. A dianionic reagent similar to B would be preferred since the preformed ligand could be incorporated into complexes by metathetical procedures. Herein we report the first such synthesis for a series of metal complexes, which defines periodic trends in the interaction between the $\mathrm{N_4R_2}$ unit and a transition metal. A portion of this work has been communicated previously.[4]

Experimental Section

Reactions were performed with standard Schlenk and cannula filtration techniques using a nitrogen atmosphere. Solids were manipulated under nitrogen in a Vacuum Atmospheres glovebox equipped with an HE-493 Dri-Train. Glassware was flame-dried before use. Hydrocarbon solvents were refluxed over sodium benzophenone ketyl and distilled under nitrogen. Benzene and tetrahydrofuran solvents were refluxed over potassium benzophenone ketyl and distilled under nitrogen. Phenyl azide,[5a] $\mathrm{NiCl_2(PPh_2Me)_2}$,[5b] $\mathrm{PdCl_2(PEt_3)_2}$,[5b] and $\mathrm{PtCl_2(PEt_3)_2}$[5b] were prepared by literature methods. (*Caution*! Phenyl azide is explosive; exposure to acid or heavy metals should be avoided.) The phenyl azide was stored and used as a 2–3 M toluene solution. The concentration of $\mathrm{PhN_3}$ in toluene was determined by a modified iodometry procedure.[5c] To 25 mL of HI were added 1.0 mL of $\mathrm{PhN_3}$ in toluene, 5 mL of $\mathrm{CCl_4}$ (or 5 mL of $\mathrm{CS_2}$), and 10 mL of a saturated KI solution. ($\mathrm{CCl_4}$ or $\mathrm{CS_2}$ was added to reduce the formation of a charge-transfer complex between toluene and $\mathrm{I_2}$.) After it was stirred for 0.5 h, the solution was titrated with standardized $\mathrm{Na_2S_2O_3}$ with starch as an indicator.

Cyclic voltammetric studies were carried out by using a BAS 100 electrochemical analyzer equipped with a Houston Instruments DMP-40 plotter. Solutions (THF) were ca. 1 mM in the metal complex and contained 0.1 M tetrabutylammonium tetrafluoroborate supporting electrolyte. For these measurements, a conventional three-electrode cell (Pt-disk working electrode, Pt-wire auxiliary electrode; Ag-wire pseudo reference electrode) was employed. Instrumental iR compensation was applied in all measurements. The $E^{\circ\prime}$ value for the $\mathrm{Cp_2Fe/Cp_2Fe^+}$ couple was 0.72 V at 500 mV/s in this cell. IR spectra were recorded with a Perkin-Elmer 1330 spectrometer or an IBM IR32 FTIR spectrometer. UV spectra were recorded with an IBM UV9420 spectrometer. Elemental analyses were performed by Schwarzkopf Microanalytical Laboratory.

Synthesis of $\mathrm{[Li(THF)_x]_2[PhNN{=}NNPh]}$ (1). A solution of LiNHPh was prepared by adding 10.3 mL of 1.6 M n-BuLi (16.5 mmol) in hexane to 1.5 mL (16.5 mmol) of aniline in 25 mL of THF. To this solution was added 7.8 mL (16.5 mmol) of 2.17 M $\mathrm{PhN_3}$[5c] in toluene, and an unstable yellow solid, $\mathrm{[Li(THF)_x][N(Ph)NNNH(Ph)]}$, formed. After 1 h 30.9

---

(1) (a) University of California at San Diego. (b) Nicolet Instrument Corp.

(2) (a) Gross, M. E.; Trogler, W. C.; Ibers, J. A. *J. Am. Chem. Soc.* **1981**, *103*, 192–193. (b) Overbosch, P.; van Koten, G.; Overbeek, O. *ibid.* **1980**, *102*, 2091–2093. (c) Doedens, R. J. *Chem. Commun.* **1968**, 1271–1272. (d) Einstein, F. W. B.; Sutton, D. *Inorg. Chem.* **1972**, *11*, 2827–2831. (e) Overbosch, P.; van Koten, G.; Grove, D. M.; Spek, A. L.; Duisenberg, A. J. M. *ibid.* **1982**, *21*, 3253–3260. (f) Overbosch, P.; van Koten, G.; Spek, A. L.; Roelofsen, G.; Duisenberg, A. J. M. *ibid.* **1982**, *21*, 3908–3913. (g) Cenini, S.; Fantucci, P.; La Monica, G. *Inorg. Chim. Acta* **1975**, *13*, 243–245. (h) La Monica, G.; Sondrinic, P.; Zingales, F.; Cenini, S. *J. Organomet. Chem.* **1973**, *50*, 287–296. (i) Trogler, W. C.; Johnson, C. E.; Ellis, D. E. *Inorg. Chem.* **1981**, *20*, 980–986. (j) Gross, M. E.; Trogler, W. C. *J. Organomet. Chem.* **1981**, *209*, 407–414. (k) Johnson, C. E.; Trogler, W. C. *J. Am. Chem. Soc.* **1981**, *103*, 6352–6358.

(3) Inagaki, G.; Goto, N. J. *J. Am. Chem. Soc.* **1987**, *109*, 3234–3240.

(4) Lee, S. W.; Miller, G. A.; Campana, C. F.; Maciejewski, M. L.; Trogler, W. C. *J. Am. Chem. Soc.* **1987**, *109*, 5050–5051.

(5) (a) Lindsay, R. O.; Allen, C. F. H. *Organic Synthesis*; Wiley: New York, 1955; Collect. Vol. IV, p 710. (b) Royle, J. R.; Slade, P. E.; Jonassen, H. B. *Inorg. Synth.* **1960**, *6*, 218. (c) Leffler, J. E.; Tsuno, Y. *J. Org. Chem.* **1963**, *28*, 190–194. Carpenter, W. R. *Anal. Chem.* **1964**, *36*, 2352–2353.

0020-1669/88/1327-1215$01.50/0

Table I. Crystallographic Data and Summary of Data Collection and Structure Refinement

	II	III	IV
formula	$C_{38}H_{36}N_4P_2Ni$	$C_{24}H_{40}N_4P_2Pd$	$C_{24}H_{40}N_4P_2Pt$
fw	669.395	552.94	641.71
cryst color	black	green-black	red
cryst syst	monoclinic	monoclinic	tetragonal
space group	$C2/c$	$P2_1/c$	$P\bar{4}2_1c$
a, Å	23.556 (3)	12.904 (3)	12.253 (1)
b, Å	9.044 (1)	13.405 (4)	
c, Å	17.829 (3)	16.670 (4)	17.803 (4)
β, deg	114.70 (3)	112.01 (3)	
V, Å^3	3462 (1)	2673 (2)	2671 (1)
Z	4	4	4
d_{calcd}, g cm^{-3}	1.28	1.37	1.60
cryst dimens, mm	0.2 × 0.4 × 0.7	0.3 × 0.2 × 0.2	0.3 × 0.3 × 0.1
μ, cm^{-1}	6.52	7.9	54.1
scan type	$\theta/2\theta$	ω	$\theta/2\theta$
scan rate	variable	variable	variable
2θ range, deg	3–40	3–45	3–40
no. of unique data	3342	2136	1016
no. of rflns used ($I > 3\sigma(I)$)	1409	1111	695
no. of params	163	141	72
R	0.055	0.050	0.044
R_w	0.055	0.043	0.059

mL (49.5 mmol) of more of the *n*-BuLi solution was added slowly and the mixture stirred for 1 h. The yellow slurry of $[Li(THF)_x]_2[PhN_4Ph]$ (I) was filtered by using Schlenk techniques, and the precipitate was washed with four 20-mL portions of pentane. The resulting pyrophoric yellow solid (4.70 g) was dried under vacuum and stored under N_2. Complex I exhibits a slight solubility in THF and benzene, but decomposition takes place in acetone, CH_2Cl_2, $CHCl_3$, CCl_4, H_2O, and CH_3OH. Addition of H_2O decomposed I into $PhNH_2$ and PhN_3, which was confirmed by NMR and IR spectral analyses. The number of coordinated THF molecules in I was determined to be about 3 from the NMR study. This number, however, was dependent on the duration of vacuum drying and the experimental scale.

Synthesis of (1,4-Diphenyltetrazenido)bis(diphenylmethylphosphine)nickel, $Ni(1,4\text{-}Ph_2N_4)(PPh_2Me)_2$ (II). Addition of 0.13 g of I in 15 mL of benzene to a stirred red solution of 0.3 g (0.57 mmol) of $NiCl_2(PPh_2Me)_2$ in 15 mL of benzene gave a dark orange solution after 6 h. The solution was filtered, concentrated under vacuum, and layered with pentane to yield (0.1 g, 26%) black crystals of II. ^1H NMR (C_6D_6): δ 7.13 (s, C_6H_5), 1.43 (d, $^2J_{P-H}$ = 14 Hz, CH_3). Anal. Calcd for $C_{38}H_{36}N_4P_2Ni$: C, 68.18; H, 5.42; N, 8.37. Found: C, 68.4; H, 5.18; N, 8.49. Mp: 128–130 °C with liberation of gas. d_{obsd}: 1.28 g cm^{-3} (CCl_4/pentane).

Synthesis of (1,4-Diphenyltetrazenido)bis(triethylphosphine)palladium(II), $Pd(1,4\text{-}Ph_2N_4)(PEt_3)_2$ (III). Addition of 0.2 g of I in 15 mL of benzene to a stirred suspension of 0.3 g (0.73 mmol) of *cis*-$PdCl_2(PEt_3)_2$ in 15 mL of benzene gave a dark green solution after 5 h. This solution was filtered, concentrated, and layered with pentane to yield (0.16 g, 40%) green-black crystals of III. ^1H NMR (C_6D_6): δ 7.23 (s, C_6H_5), 1.13 (m, J_{H-H} = 7 Hz, J_{P-H} = 36 Hz, CH_2), 0.67 (t, J = 6 Hz, CH_3). $^{31}P\{^1H\}$ NMR (C_6D_6): δ 60.3 (s). Anal. Calcd for $C_{24}H_{40}N_4P_2Pd$: C, 52.1; H, 7.29; N, 10.1. Found: C, 51.7; H, 7.03; N, 9.63. Mp: 122–124 °C with liberation of gas.

Synthesis of (1,4-Diphenyltetrazenido)bis(triethylphosphine)platinum(II), $Pt(1,4\text{-}Ph_2N_4)(PEt_3)_2$ (IV). Addition of 0.15 g of I in 30 mL of benzene to a stirred slurry of 0.33 g (0.66 mmol) of $PtCl_2(PEt_3)_2$ in 30 mL of benzene gave a red solution. After 12 h this solution was filtered, concentrated, and layered with pentane to yield (0.15 g, 36%) red crystals of IV. ^1H NMR (C_6D_6): δ 7.26 (s, C_6H_5), 1.31 (m, J_{H-H} = 7 Hz, J_{P-H} = 48 Hz, CH_2), 0.78 (t, J = 7 Hz, CH_3). $^{31}P\{^1H\}$ NMR (C_6D_6): δ 39.2 (J_{Pt-P} = 3355 Hz). Anal. Calcd for $C_{24}H_{40}N_4P_2Pt$: C, 44.9; H, 6.28; N, 8.73. Found: C, 44.8; H, 5.92; N, 7.92. Mp: 175–177 °C with liberation of gas.

X-ray Structure Determination. All X-ray data were collected with use of a Nicolet R3/μ automated diffractometer equipped with a Mo X-ray tube and a graphite-crystal monochromator. Details on crystal data and intensity data are given in Table I. The orientation matrix and unit cell parameters were determined from 25 machine-centered reflections with 15 < 2θ < 30°. Intensities of three check reflections were monitored after every 100 reflections during data collection. The scan width used in intensity data collection was 0.5° below $K\alpha_1$ to 0.5° above $K\alpha_2$. Data were corrected for Lorentz and polarization effects. No absorption correction was applied except for the platinum complex (IV). All calculations were carried out on a Microvax II computer with use of the SHELXTL PLUS program package.

A black hygroscopic crystal of II, shaped as a plate, of approximate dimensions 0.2 × 0.4 × 0.7 mm, was affixed in a glass capillary for crystal data and intensity data collection. The unit cell parameters and systematic absences hkl ($h + k = 2n + 1$), $h0l$ ($l = 2n + 1$), and $0k0$ ($k = 2n + 1$) indicated two possible space groups: Cc and $C2/c$. The structure was solved first in the Cc space group by locating the Ni atom by direct methods. Several carbon atoms were located by Fourier and difference Fourier syntheses and least-squares refinements. After a few cycles of refinement it was apparent that the procedure failed to converge. The $C2/c$ space group was then used, locating the Ni atom at a special position on the C_2 axis. Subsequent difference syntheses revealed all non-hydrogen atoms. Isotropic refinement of all non-hydrogen atoms converged in this space group to R = 0.084. The subsequent anisotropic refinements of Ni, P, and N atoms converged to R = 0.062, and difference Fourier synthesis revealed all hydrogen atoms. Finally, three cycles of accelerated full-matrix least-squares refinements in which all hydrogen isotropic thermal parameters were fixed converged to R = 0.055. All residual peaks in the last difference Fourier map were less than 0.7 e Å^{-3}.

A green-black crystal of III, shaped as a block of approximate dimensions 0.3 × 0.2 × 0.2 mm, was used for crystal and intensity data. The systematic absences $h0l$ ($l = 2n + 1$) and $0k0$ ($k = 2n + 1$) unambiguously indicated $P2_1/c$ as the space group. The structure was solved by direct methods, and the Pd and P atoms were included anisotropically in the structure refinement. The final R value was 0.050.

A red prism of IV, of approximate dimensions 0.3 × 0.3 × 0.2 mm, was used for structure determination. The systematic absences hhl ($l = 2n + 1$) and $h00$ ($h + 2n = 1$) unambiguously indicated $P\bar{4}2_1c$. The structure was solved by locating the Pt and P atoms by direct methods and other non-hydrogen atoms from subsequent difference Fourier syntheses. The Pt and P atoms were included anisotropically in the structure refinement. The final R value was 0.044.

Final atomic positional parameters for non-hydrogen atoms are shown in Table II; anisotropic thermal parameters, complete tables of bond distances and angles, hydrogen atom coordinates, and tables of observed and calculated structure factors are available as supplementary material.

Results and Discussion

A convenient entry to the synthesis of the tetrazenido ligand was attained by the addition of lithium anilide to phenyl azide, followed by addition of an excess of *n*-BuLi to generate the isolable dianion (eq 1). This highly reactive, air-sensitive dianion undergoes fragmentation to phenyl azide and aniline on addition of protic species such as water and methanol. It is also a useful reagent for the synthesis of tetraazadiene (or tetrazenido) complexes by simple metathetical procedures, as outlined in eq 2.

$$\mathrm{LiNPhH + N_3Ph \xrightarrow[THF]{} LiN(Ph)N{=}NN(Ph)H \xrightarrow{3\textit{n}\text{-}BuLi}}$$
$$\mathrm{LiN(Ph)N{=}NN(Ph)Li}\downarrow \quad (1)$$

All three 1,4-diphenyltetrazenido complexes of bis(phosphine)nickel, -palladium, and -platinum were synthesized by the reaction between I and the precursor dichlorobis(phosphine)metal complexes (eq 2). We could not synthesize the bis(phosphine)metal–tetraazadiene complexes from precursors such as $NiCl_2(PMe_3)_2$ or $NiCl_2(PEt_3)_2$, probably because the configuration of these dihalides is trans square planar.[6] The complex $NiCl_2(Ph_2MeP)_2$ is, however, in equilibrium between a trans square plane and a tetrahedral structure. This suggests that the synthesis requires a cis or tetrahedral dihalometal complex.

$$\mathrm{L_2MCl_2 + [Li(THF)_{\mathit{x}}]_2[N(Ph)N{=}NNPh] \rightarrow}$$
$$\overline{\mathrm{M(N(Ph)N{=}N}}\mathrm{NPh)L_2 + 2LiCl} + x\mathrm{THF} \quad (2)$$

II: $L = PPh_2Me$, $M = Ni$
III: $L = PEt_3$, $M = Pd$
IV: $L = PEt_3$, $M = Pt$

Molecular Structures of II–IV. The molecular structures with atomic numbering schemes are shown in Figures 1–3. All three molecules have a molecular C_2 axis passing through the metal,

---

(6) (a) Tolman, C. A. *Chem. Rev.* **1977**, *77*, 313–348. (b) Klein, H.-F. *Angew. Chem., Int. Ed. Engl.* **1980**, *19*, 362–375.

Table II. Atomic Coordinates (×10^4) and Isotropic Temperature Factors (×10^3 Å^2)

	x	y	z	U(eq)^a		x	y	z	U(eq)^a
				Ni(1,4-Ph$_2$N$_4$)(PPh$_2$Me)$_2$ (II)					
Ni	5000	935 (1)	2500	39 (1)	C(101)	5787 (3)	−593 (8)	4043 (4)	48 (2)
P(1)	4203 (1)	2427 (2)	2085 (1)	42 (1)	C(102)	5745 (3)	292 (9)	4620 (5)	58 (2)
N(1)	5306 (2)	−652 (6)	3236 (3)	46 (3)	C(111)	4318 (4)	6054 (10)	3541 (5)	70 (2)
C(11)	3485 (3)	1395 (8)	1888 (4)	44 (2)	C(16)	2899 (4)	1938 (11)	1386 (6)	80 (3)
C(12)	3531 (3)	74 (9)	2293 (5)	54 (2)	C(110)	4303 (3)	5416 (9)	4228 (5)	62 (2)
C(17)	4230 (3)	3652 (7)	2908 (4)	40 (2)	C(113)	4014 (5)	3662 (10)	1215 (6)	64 (2)
C(13)	2988 (4)	−736 (10)	2188 (5)	71 (2)	C(103)	6213 (4)	322 (10)	6405 (6)	74 (3)
C(18)	4226 (3)	3028 (9)	3617 (5)	51 (2)	C(104)	6712 (4)	−624 (11)	5651 (6)	80 (3)
C(19)	4262 (3)	3930 (9)	4272 (5)	61 (2)	C(15)	2362 (5)	1098 (12)	1289 (6)	98 (3)
C(112)	4285 (3)	5174 (9)	2878 (5)	59 (2)	C(106)	6303 (4)	−1665 (9)	4296 (5)	64 (2)
C(14)	2420 (5)	−165 (11)	1701 (6)	84 (3)	C(105)	6750 (4)	−1606 (10)	5089 (6)	74 (3)
N(2)	5201 (3)	−2014 (6)	2891 (3)	58 (3)					
				Pd(1,4-Ph$_2$N$_4$)(PEt$_3$)$_2$ (III)					
Pd	2100 (1)	2417 (1)	2785 (1)	33 (1)	C(13)	−203 (12)	2371 (12)	1175 (8)	31 (4)
P(1)	1090 (4)	1357 (3)	3293 (3)	36 (2)	C(14)	−997 (12)	2637 (13)	1508 (8)	41 (4)
C(1)	321 (13)	435 (10)	2477 (9)	43 (5)	C(15)	−2095 (13)	2347 (13)	1104 (9)	56 (5)
C(2)	1050 (14)	−44 (12)	2033 (10)	68 (6)	C(16)	−2399 (15)	1788 (12)	342 (11)	62 (6)
C(3)	56 (13)	1883 (11)	3696 (10)	55 (5)	C(17)	−1659 (15)	1495 (12)	9 (11)	64 (6)
C(4)	−1016 (13)	1323 (12)	3515 (10)	65 (6)	C(18)	−529 (14)	1802 (11)	409 (9)	51 (5)
C(5)	1985 (13)	591 (12)	4191 (9)	57 (5)	N(2)	1302 (12)	3032 (9)	971 (7)	46 (4)
C(6)	1427 (14)	−105 (12)	4638 (10)	69 (6)	N(3)	2334 (12)	3214 (10)	1242 (8)	54 (4)
P(2)	3294 (4)	2966 (3)	4118 (2)	40 (2)	N(4)	2969 (11)	2853 (7)	2044 (7)	36 (4)
C(7)	4146 (12)	4030 (10)	4033 (9)	39 (5)	C(19)	4131 (14)	3048 (12)	2249 (9)	41 (5)
C(8)	3463 (14)	4885 (12)	3480 (10)	68 (6)	C(20)	4853 (14)	2298 (13)	2680 (9)	50 (5)
C(9)	4306 (13)	2223 (12)	4977 (9)	63 (6)	C(21)	6006 (14)	2433 (16)	2899 (9)	69 (5)
C(10)	4957 (15)	1464 (12)	4723 (10)	73 (6)	C(22)	6368 (16)	3292 (13)	2672 (10)	68 (6)
C(11)	2469 (13)	3498 (12)	4692 (10)	57 (5)	C(23)	5659 (15)	4025 (13)	2251 (10)	62 (6)
C(12)	3084 (13)	4056 (12)	5538 (9)	64 (6)	C(24)	4503 (15)	3911 (12)	2010 (9)	52 (5)
N(1)	891 (10)	2703 (10)	1585 (7)	41 (4)					
				Pt(1,4-Ph$_2$N$_4$)(PEt$_3$)$_2$ (IV)					
Pt(1)	5000	0	1038 (1)	26 (1)	N(1)	5523 (13)	860 (13)	1919 (10)	36 (5)
P(1)	6149 (4)	724 (4)	177 (3)	32 (2)	N(2)	5275 (13)	462 (13)	2637 (9)	39 (5)
C(1)	6492 (15)	−261 (16)	−580 (11)	44 (6)	C(7)	5097 (16)	1873 (16)	1994 (10)	27 (5)
C(2)	7491 (16)	−44 (19)	−1045 (9)	43 (5)	C(8)	7057 (19)	1951 (21)	2433 (17)	57 (6)
C(3)	5784 (17)	1950 (16)	−360 (12)	44 (6)	C(9)	7640 (20)	2926 (17)	2455 (15)	41 (7)
C(4)	6602 (19)	2856 (21)	−480 (15)	68 (8)	C(10)	7328 (23)	3762 (22)	2031 (14)	74 (8)
C(5)	7482 (15)	1028 (14)	586 (11)	34 (5)	C(11)	6368 (25)	3718 (25)	1617 (16)	78 (9)
C(6)	7958 (17)	105 (19)	978 (10)	42 (5)	C(12)	5724 (18)	2754 (18)	1576 (11)	45 (6)

^{a}Denotes equivalent isotropic U, defined as one-third of the trace of the orthogonalized $\mathbf{U}_{ij}$ tensor.

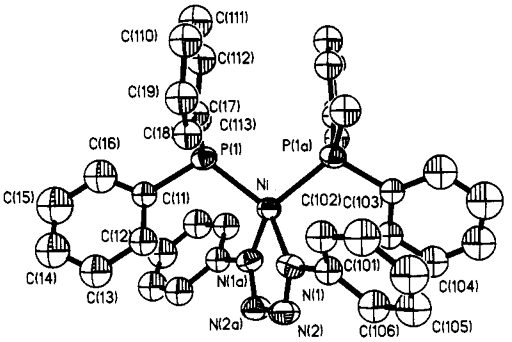

Figure 1. ORTEP drawing of compound II showing the atom-labeling scheme and 50% probability thermal ellipsoids. The view is perpendicular to the plane containing the metal and two phosphine atoms. Unlabeled atoms are related to labeled atoms by the crystallographic C_2 axis bisecting the metallacycle ring.

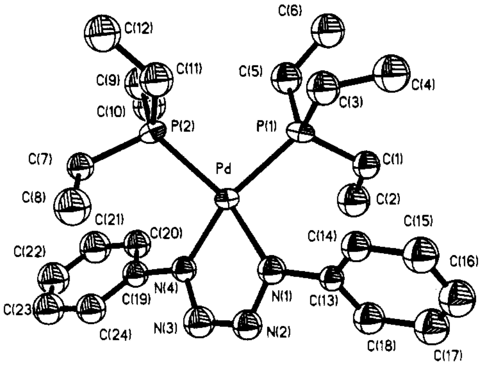

Figure 2. ORTEP drawing of compound III showing the atom-labeling scheme and 50% probability thermal ellipsoids. The view is perpendicular to the plane containing the metal and two phosphine atoms.

bisecting the N(2)–N(2a) bond. For II and IV this axis coincides with a crystallographic C_2 axis. The coordination sphere of II can be described as a tetrahedron distorted toward a square plane (Figure 1) with a dihedral angle of 56.9° between the planes defined by the metallacycle and NiP$_2$ fragment. The coordination sphere of the palladium and platinum complexes can be described as a square plane distorted toward a tetrahedral structure (Figures 2 and 3 and Table III) with corresponding dihedral angles of 36.6 and 26.6°, respectively. In all compounds the metallacycle ring adopts a nearly planar geometry with the average displacement of an atom from the least-squares planes being less than 0.045 Å. All phenyl rings on the metallacycles are twisted out of the plane of the metallacycle ring and are mutually perpendicular (95–99°). The equations of the least-squares plane of the metallacycle and the MP$_2$ fragment and their dihedral angles are given in Table III.

Of particular interest are the bonds within the metallacycle. A comparison of bond distances and bond angles within several related metallacycles is given in Table IV. In structure II, the three N–N bond distances, N(1)–N(2) (1.353 (7) Å), N(2)–N(2a) (1.321 (11) Å), and N(1a)–N(2a) (1.353 (7) Å), are almost equal. This suggests a bonding mode intermediate between the tetraazadiene (A) and tetrazenido (B) resonance structures. Extremely short Ni–N(1) and Ni–N(1a) (1.876 (5) Å) bond distances and the planarity of the metallacycle provide evidence for Ni–N π

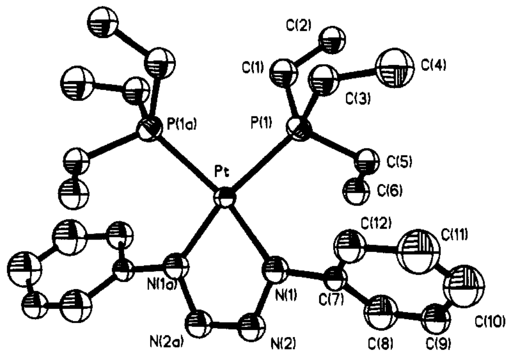

Figure 3. ORTEP drawing of compound IV showing the atom-labeling scheme and 50% probability thermal ellipsoids. The view is perpendicular to the plane containing the metal and two phosphine atoms. Unlabeled atoms are related to labeled atoms by the crystallographic C_2 axis bisecting the metallacycle ring.

Table III. Least-Squares Planes in Complexes II–IV

Least-Squares Planes

plane no.	atoms in plane	eq of planes[a]				av displacement, Å
		A	*B*	*C*	*D*	
1	NiN_4	23.211	0.00	−10.146	9.0692	0.042
2	NiP_2	−9.294	0.00	17.886	−0.1755	0
3	PdN_4	−2.486	12.549	5.751	4.0840	0.045
4	PdP_2	−8.626	9.958	3.623	1.6042	0
5	PtN_4	10.482	−6.344	0.00	5.2407	0.003
6	PtP_2	−6.532	10.365	0.00	−3.2662	0

Dihedral Angles between Planes

plane no.		angle, deg
1	2	56.9
3	4	36.6
5	6	26.6

[a] These equations are of the form $Ax + By + Cz = D$.

back-bonding, since a metal–nitrogen single bond is expected to lie within 1.95–2.15 Å.[7] Three N–N bond distances in $((3,5\text{-}Me_2C_6H_3)N_4(3,5\text{-}(Me_2C_6H_3))_2Ni$[2b] are also equivalent (see Table IV), but evidence for metal–nitrogen π bonding was not clear because of strong conjugation with coplanar aryl substituents in that structure. The complex $(\eta^5\text{-}C_5H_5)Co((C_6F_5)N_4(C_6F_5))$ was the first to show pronounced metal–nitrogen π bonding from the metal $d(\pi) \rightarrow N_4(\pi^*)$ interaction.[2a] Considering the diamagnetism of II and its tetrahedral geometry, the complex is best viewed as a Ni(0) complex of the neutral tetraazadiene ligand.

In structure III, the N(2)–N(3) bond distance of 1.26 (2) Å is significantly shorter than the N(1)–N(2) (1.39 (1) Å) and N(3)–N(4) (1.37 (1) Å) bonds; the last two are equivalent within the experimental error. These bond distances correspond to one double and two single nitrogen–nitrogen bonds.[8] The Pd–N(1) (2.06 (1) Å) and Pd–N(4) (2.04 (1) Å) distances indicate Pd–N single bonds. The structural data for III show the PdN_4 metallacycle conforms to structure B, in which the tetrazenido ligand acts as a four-electron σ donor to Pd(II).

In structure IV the N(2)–N(2a) bond distance of 1.32 (2) Å is shorter than the N(1)–N(2) and N(1a)–N(2a) (1.40 (2) Å) bonds. These distances also suggest one double and two single nitrogen–nitrogen bonds. The Pt–N(1) and Pt–N(1a) bond distances of 2.00 (2) Å suggest Pt–N single bonds. The structural data best fit the picture of Pt(II) in a square-planar environment bound to the tetrazenido ligand.

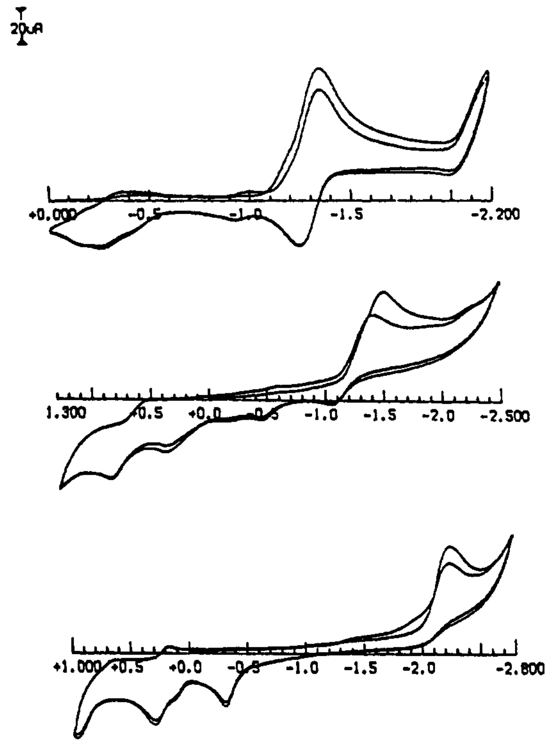

Figure 4. Cyclic voltammograms (500 mV/s) in 0.1 M Bu_4NBF_4–THF solutions of II (top), III (middle), and IV (bottom).

Several trends are evident in the comparative structural studies. First, the distortion from a square-planar M(II) complex increases greatly along the series Pt, Pd, Ni such that the Ni complex assumes a structure consistent with tetrahedral Ni(0). Alternatively, the complex can be viewed as a low-spin tetrahedral Ni(II) complex because of a large splitting in the uppermost t_2-derived d orbitals. The structural change between Pd and Pt cannot be attributed to steric effects; however, the severe distortion from a square-planar geometry in the Ni derivative may partly reflect increased steric strain resulting from the shortened Ni–N distances. Second, the degree of back-bonding to the N_4R_2 ligand is much greater for Ni than for the Pd and Pt analogues as evidenced by the metrical parameters within the NiN_4 unit. Third, the N–M–N bond angles in these and other complexes (Table IV) lie between 71 and 80°, which suggests angle strain in the metallacycle fragment. The narrow bite of the N_4R_2 ligand is best accommodated in first-row-metal complexes. These structural results emphasize the flexible electron donor–acceptor properties of the tetraazadiene ligand.

Electronic Absorption Spectra. The dianionic ligand I displays a weak low-energy maximum at 407 nm, which rapidly decreases on exposure to the spectrophotometer light source (see Table V). This absorption can be assigned to a forbidden $n \rightarrow \pi^*$ transition similar to that of azobenzene.[9] The nickel complex II shows two energy maxima at 299 and 440 nm, which are assigned to a combination of a metallacycle $\pi \rightarrow \pi^*$ transition and a $d \rightarrow \pi^*$ transition. These assignments resemble those proposed[10] for $CpCo(1,4\text{-}H_2N_4)$ on the basis of SCF-Xα-DV molecular orbital calculations. The lower energy absorption (780 nm) might be assigned to ligand-field transition (d–d transition if Ni(II)). The palladium complex III displays three energy maxima at 324, 394, and 612 nm. The two higher energy transitions (324, 394 nm) can be assigned to a mixture of d → metallacycle π^* and metallacycle $\pi \rightarrow {}^*\pi$ transitions. Note that the band maxima (Table V) are insensitive to solvent polarity, thereby ruling out a pure

---

[7] Davis, B. R.; Payne, N. C.; Ibers, J. A. *Inorg. Chem.* **1969**, *8*, 2719–2728.

[8] (a) A few comparisons may be found in *trans*-tetrazene, $H_2N{-}N{=}N{-}NH_2$ (N—N = 1.43 (1) Å; N=N = 1.21 (2) Å): Veith, Von M.; Schlemmer, G. *Z. Anorg. Allg. Chem.* **1982**, *494*, 7–19. (b) Comparisons may also be found in tetrakis(trimethylsilyl)tetrazene (N—N = 1.394 (5) Å; N=N = 1.268 (7) Å): Veith, Von M. *Acta Crystallogr. Sect. B: Struct. Crystallogr. Cryst.* **1975**, *B31*, 678–684.

[9] Geoffroy, G. L.; Wrighton, M. S. *Organometallic Photochemistry*; Academic: New York, 1979.

[10] Maroney, M. J.; Trogler, W. C. *J. Am. Chem. Soc.* **1984**, *106*, 4144–4151.

Table IV. Bond Distances (Å) and Bond Angles (deg) within the Metallacycles in Related Complexes, $\overline{\text{M–N(1)–N(2)–N(2a)–N(1a)}}$[a]

complex	M–N(1), M–N(1a)	N(1)–N(2), N(1a)–N(2a)	N(2)–N(2a)	N(1)–M–N(1a)	M–N(1)–N(2), M–N(1a)–N(2a)	N(1)–N(2)–N(2a), N(1a)–N(2a)–N(2)	ref
$Ni(PhN_4Ph)(PPh_2Me)_2$	1.876 (5), 1.876 (5)	1.353 (7), 1.353 (7)	1.321 (11)	80.1 (6)	116.3 (3), 116.3 (3)	113.9 (4), 113.9 (4)	this work
$Pd(PhN_4Ph)(PEt_3)_2$	2.06 (1), 2.04 (1)	1.39 (1), 1.37 (1)	1.26 (1)	75.4 (5)	114.5 (9), 115.4 (10)	116.6 (13), 116.2 (13)	this work
$Pt(PhN_4Ph)(PEt_3)_2$	2.00 (2), 2.00 (2)	1.40 (2), 1.40 (2)	1.32 (2)	76.4 (6)	117.6 (12), 117.6 (12)	114.2 (10), 114.2 (10)	this work
$(\eta^5\text{-}C_5H_5)Co((C_6F_5)N_4(C_6F_5))$	1.819 (2), 1.802 (2)	1.355 (2), 1.360 (2)	1.279 (2)	79.01 (7)	118.1 (1), 118.6 (1)	112.2 (2), 112.1 (2)	2a
$Ni((3,5\text{-}Me_2C_6H_3)N_4(3,5\text{-}Me_2C_6H_3))_2$	1.853 (3), 1.853 (3)	1.325 (3), 1.325 (3)	1.319 (3)	79.5 (1)	116.8 (2), 116.8 (2)	113.5 (2), 113.5 (2)	2b
$Fe(Me_2N_4)(CO)_3$	1.83 (3)		1.32 (3)[b]				2c
$Ir((4\text{-}FC_6H_4)N_4(4\text{-}FC_6H_4))(CO)(PPh_3)$	1.94 (1), 1.97 (1)	1.35 (2), 1.40 (2)	1.27 (2)	74.0 (5)	119.6 (9), 119.7 (9)	112.2 (12), 114.2 (12)	2d
$Pt((4\text{-}NO_2C_6H_4)N_4(4\text{-}NO_2C_6H_4))\text{-}(\overline{CHC(PEt_3)H(CH_2)_2CH{=}CHCH_2CH_2})(PEt_3)$	2.169 (5), 2.159 (5)	1.385 (7), 1.391 (7)	1.263 (8)	71.5 (2)	116.0 (4), 116.4 (4)	117.3 (5), 117.0 (5)	2e
$(\eta^5\text{-}C_5H_5)Ni((4\text{-}MeC_6H_4)N_4(4\text{-}MeC_6H_4))$	1.853 (2), 1.843 (2)	1.344 (2), 1.346 (2)	1.278 (2)	80.43 (7)	114.9 (1), 115.7 (1)	114.9 (2), 113.6 (2)	2f

[a] See Figure 1. [b] The average of three N–N bond distances.

Table V. Electronic Absorption Spectra of Complexes I–IV

complex	solvent	λ_{max}, nm	ε, $M^{-1}\ cm^{-1}$
I	THF	407	25[a]
II[b]	THF	~300	~39000
		440	~2300
		780	~460
III[b]	C_6H_6	324	27000
		394	9100
		612	1700
IV	THF	339	16000
		473	1800
	C_6H_6	337	15000
		475	1700

[a] I rapidly decomposed (ca. 20 min) on the repetitive scans. [b] III decomposed (ca. 3 h) in THF so the peak intensities may not be accurate.

Table VI. Electrochemical Data from Cyclic Voltammetry Studies of Complexes II–IV[a]

compd	scan rate, mV/s	$E°$,[b] V	ΔE_p,[c] mV	I_{p_a}/I_{p_c}	E_{p_c}, V	E_{p_a}, V
II	3000	−1.09	173	0.95		
	1000	−1.12	144	0.89		
	500	−1.19	127	0.92		
	200	−1.25	108	0.96		
	100	−1.28	97	0.73		
	50	−1.27	99	0.67		
III[d]	500				−1.45	−1.07 −0.46 0.38
IV[d]	500				−2.23	−1.19 −0.31

[a] Recorded in 1 mM THF solutions containing 0.1 M $n\text{-}Bu_4NBF_4$. [b] Vs Ag pseudoreference. [c] With *iR* compensation. [d] Data taken from +1.3 V to −2.8 V scans. These processes are irreversible.

d → ligand π* charge-transfer assignment. The extinction coefficients (27 000, 9100 $M^{-1}\ cm^{-1}$) suggest that these transitions are of ligand or charge-transfer origin. The lowest energy transition is again assigned to a d–d transition. With use of the same strategy employed for complex III, a higher energy transition in IV can be assigned to a d → π* transition and a lower one to a d–d transition. The increasing size of the crystal field slitting as one descends a triad in the periodic table agrees with the above data: II > III > IV for the charge-transfer bands and II < III < IV for the d–d localized absorptions. The pseudotetrahedral structure of complex II also accounts for the low energy of the d–d transition (737 nm) since the crystal field splitting decreases on distortion toward a tetrahedral geometry. If II is to be regarded as a formally Ni(0) complex, then the long-wavelength "d–d" transition is better viewed as a forbidden d → metallacycle π* transition. As noted earlier, the oxidation-state formalism breaks down for metal complexes of the covalent tetraazadiene ligand. All the complexes decomposed slowly when irradiated in the 290–350-nm charge-transfer absorption region.

Electrochemistry. Complex II displays a chemically reversible reduction in its cyclic voltammogram at a potential of −1.11 V vs a Ag-wire pseudoreference, whereas complexes III and IV display chemically irreversible reductions (Figure 4 and Table VI). At slow scan rates (Table VI) the reduction of II becomes chemically irreversible, which suggests the anion radical is unstable. The ease of reduction parallels the energy of the lowest electronic excited state in these complexes (Table V).

Acknowledgment. This work is based on research sponsored by the Air Force Office of Scientific Research, Air Force Systems Command, USAF, under Grant AFOSR-86-0027. We thank the DoD University Research Instrumentation Program (Grant DAAL03-87-G-0071) for funds to purchase an X-ray diffractometer.

Registry No. I, 109719-16-6; II, 113056-43-2; III, 109719-15-5; IV, 113056-44-3; $NiCl_2(Ph_2MeP)_2$, 15683-37-1; *cis*-$PdCl_2(PEt_3)_2$, 77027-39-5; $PtCl_2(PEt_3)_2$, 15692-07-6; LiNHPh, 20732-26-7; PhN_3, 622-37-7.

Supplementary Material Available: Tables of bond distances, bond angles, thermal parameters, and positional parameters for hydrogen atoms for II–IV (8 pages); tables of observed and calculated structure factors (12 pages). Ordering information is given on any current masthead page.